Displacement and energy demand imposed by rapid bulking and tunnel shape change

Fedilberto J. Gonzalez
Queen's University, Miller Hall, Kingston, Ontario, Canada

Peter K. Kaiser
Laurentian University, Sudbury, Ontario, Canada

Mark S. Diederichs
Queen's University, Miller Hall, Kingston, Ontario, Canada

ABSTRACT: In burstprone ground, sudden and violent failure of hard brittle rock dynamically loads and deforms ground support. Failure of underground excavations comprises two processes: bulking of stress-fractured rock and shape changes of the excavation in response to the fracturing process. For demonstration purposes, a case with a stress ratio $k < 1$ is examined. Brittle failure of sidewalls occurs if induced stresses exceed the crack propagation stress level, leading to a rupture process and rock mass convergence in which the bulking rock moves rapidly toward the excavation. At the same time, the roof and floor converge rapidly induced by the sudden shape change due to wall rupture. This article presents estimates of kinetic energy demands that would be imposed on support by self-induced strainbursts and associated sudden and violent shape change. The effects of confining pressure at the tunnel surface on the violence of this process are explored using FLAC.

Keywords: Rapid bulking, self-induced strainburst, shape change.

1 INTRODUCTION

Deeper underground mining activities and higher production rates increase the challenges of providing a safe and productive environment for mining production as well as the development of supporting infrastructure (e.g., extraction, haulage, transport and ventilation tunnelling). Higher stresses at depth and higher production rates increase the challenges of providing a safe and productive environment. Environments at greater depths are inherently more fragile due to the increase in the stress gradient, which leads to higher differential stress (Kaiser & Moss, 2021).

A self-induced strainburst is a type of rockburst whereby part of a highly stressed volume of rock suddenly fails and causes rapid bulking deformation into the excavation without the influence of energy radiation from a distant seismic event (e.g., slip-type bursts) (Kaiser & Malovichko, 2022). The strainburst is part of the seismic source and has an implosive seismic moment tensor component (ISO), and it is referred to as a crush-type event (Malovichko, 2020).

During a self-induced strainburst, unsupported floors may also suddenly lift, and rock blocks may detach from the roof, particularly at locations experiencing low confinement or even tangential tension. These failure processes induce rapid elastic and bulking displacements with related

velocities and energy flux. These velocities are not generated by ground motions from a distant seismic event, but rather by the excavation failure process with a commonly neglected implosive (rapid closure) elastic deformation and inelastic bulking components. A well-designed rock support system must be able to survive these displacements and related kinetic energy demands.

This article presents estimates of kinetic energy flux demands by self-induced strainbursts and the sudden and violent shape change experienced by a cavity during rapid bulking. It is demonstrated that frequently observed rockburst loading conditions can be explained by sudden bulking combined with simultaneous shape-change effects. A means to estimate the support demand by pseudo-static modelling of self-induced strainbursting is provided. The effects of confining pressure at the excavation walls (support pressure) on such estimates are assessed using FLAC. The aim of this article is not to quantitatively simulate the estimation of strainburst demand, but rather to qualitatively evaluate certain factors that contribute to displacement-induced energy flux demand and its sensitivity to support pressure.

2 FORMULATION OF THE PROBLEM

Gonzalez et al. (2022) demonstrated the relevance of shape change by using an analytical solution for elliptical cavities. For the case when the in-situ stress ratio k is lower than 1 (k < 1), brittle failure of side walls occurs if induced stresses exceed the crack initiation and propagation stress level, leading to rupture process and rockmass expansion in which the bulking rock moves rapidly toward the excavation accompanied by geometric misfit of rock fragments. At the same time, the roof and floor experience rapid vertical movements induced by the sudden shape change due to wall rupture. Figure 1a shows the process of shape change. As the initially circular excavation experiences two-sided strainbursting, its geometry changes from circular to elliptical (see Figure 1b) leading to elastic inward movements on the roof and floor and possibly outward movements on the horizontal axis.

Ground motion-centric support design methods, rely primarily on relation to the intensity of distant slip-type seismic events and do not account for shape change. It is demonstrated in the following that approaches to assessing excavation damage without consideration of excavation shape changes are missing key factors that explain observed excavation and support damage. In this study, the relevance of shape change processes is highlighted using the continuum software FLAC (Itasca Consulting Group Inc., 2019).

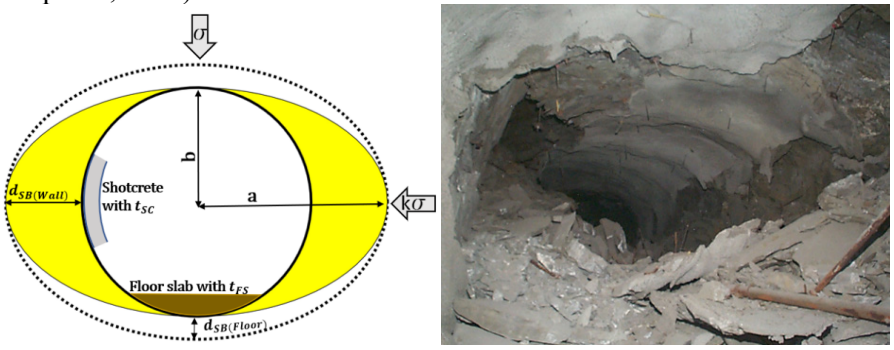

(a) (b)

Figure 1. (a) Concept of shape change (from Gonzalez et al., 2022); (b) severe excavation damage caused by two-sided strainbursting (R5 damage level) (from *Kaiser, 2016*).

2.1 Geometry set up

It is important to acknowledge the discontinuous nature of the progressive brittle failure of hard rock in deep underground excavations. To this end, six geometries representing different stages of rock fracture are modelled. The starting point is a 6 m wide circular tunnel, which is expanded in the horizontal axis, normal to the maximum principal stress, in 0.3 m increments. The zone size decreases from the excavation boundary towards the elliptical excavation to improve the stress and, as a result, the strain distribution near the tunnel.

The depth of yield in the FLAC model is assumed to correspond to the depth of bulking material by spalling or strainbursting ground. Therefore, the depth of bulking material (d_B) is simulated by the depth of yield in FLAC. Numerical simulations begin with a circular excavation. Subsequent geometries are constructed by increments of 0.3 m in the horizontal axis with a lateral extent defined by the failed zones of the initially circular excavation. This approach ensures equal lateral extent at the excavation boundary for all geometries.

2.2 Rock mass properties

The plastic-strain-dependent cohesion-weakening and frictional-strengthening model was implemented in FLAC by invoking the strain softening constitutive model (Diederichs, 2007). All simulations share these common parameters: Maximum principal stress σ_1 = 60 MPa, minimum principal stress σ_3 = 20 MPa. deformation modulus E = 30,000 MPa, Poisson's ratio υ = 0.25, peak cohesion c = 61 MPa, residual cohesion c_r = 0.5 MPa, peak friction angle ϕ = 10°, residual friction angle ϕ_r = 48°, plastic strain limit for cohesion ε_c^p = 0.2e-3, plastic strain limit for friction angle ε_ϕ^p = 0.5e-3, dilation angle Ψ = 30°, tensile strength T = 19 MPa, density ρ = 2,800 kg/m^3 and bulking duration t_B = 20 ms. This set of parameters can be calibrated using the URL Mine-by experiment from (Martin et al., 1997) as a calibration for large-grained granodiorite present at this site.

Continuum models cannot capture the geometric incompatibilities of fragments of hard rock caused by stress-driven fracture, which leads to a geometric increase in, mostly radial, displacement. The semi-empirical approach presented here uses a high dilation angle to increase high linear bulking factors, ranging from 4 to 6%. This bulking factor range, according to (Kaiser, 2016), represents conditions in mining operations with moderate HW/FW deformation and light rock support. Strictly speaking, a high dilation angle, implying isotropic dilation, does not represent the directional bulking strain and therefore is a crude approximation of the actual bulking process.

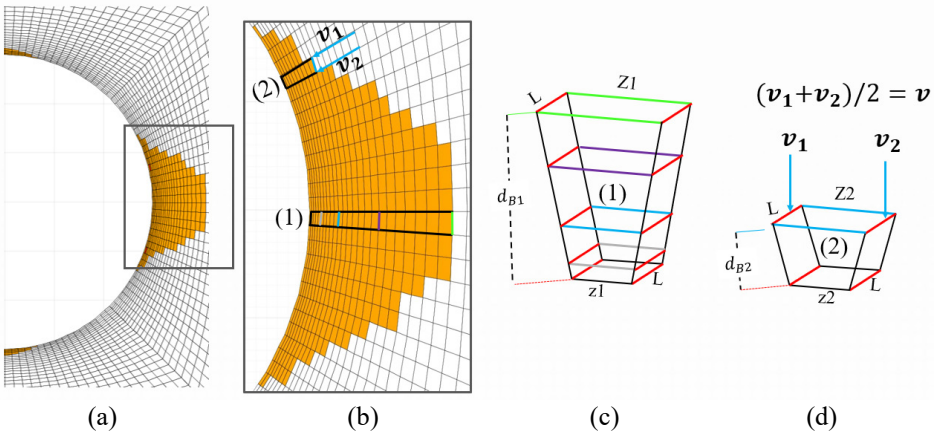

Figure 2. (a) Half-excavation depicting depth of bulking material; (b) zoom into the right sidewall; idealization of the volume to be ejected for (c) obelisk 1 and (d) obelisk 2.

2.3 Displacement and related velocities

The rock mass bulking process can be approximated by a constant linear bulking factor (BF) (Kaiser, 2016) over the depth of strainbursting. This study, however, uses displacements obtained by FLAC to reproduce the bulking process.

The shape change results in velocity vectors that represent the rate at which displacements occur during the bulking duration at the elastic material boundary. During this shape change process with k<1, there are elastic displacements imposed in the roof and floor whereas inelastic deformation is caused by the bulking material in the sidewalls. The velocity at the tunnel wall is obtained by dividing the sudden increase in wall displacement by the duration of the bulking process, i.e., the bulking duration (t_B). The bulking duration obtained from seismic waveform analyses typically ranges between 10 and 40 ms (Kaiser & Malovichko, 2022). A bulking time of 20 ms is chosen and applied here. This represents conditions of strainbursting as observed during crush-type seismic events.

2.4 *Ejected mass*

The distribution of the depth of bulking material varies along the excavation surface. Figures 2c-d show obelisk-shaped sampling volumes that are incrementally moving away from the excavation boundary with $d_{B1} > d_{B2}$. The mass of an obelisk to be ejected during the shape change process is proportional to the depth of bulking and can be estimated by Equation 1a. The rate of displacement at which each obelisk is ejected depends on the average nodal velocities $\boldsymbol{v_1}$ and $\boldsymbol{v_2}$ of each zone from the excavation boundary to the deepest depth of bulking. Calculations are presented for a unit-length along the tunnel i.e., in the out-of-plane direction.

A layer of shotcrete with a thickness of 0.3 m ($t_{sc} = 0.3\ m$) is simulated for the sidewalls and roof and a floor slab with a thickness of 0.5 m ($t_{FS} = 0.5\ m$) for the floor. The mass of shotcrete over one zone can be estimated by Equation 1b.

$$Mass\ of\ obelisk = \frac{d_B}{2}(L(z+Z))\ \rho\ ; \tag{1a}$$

$$Mass\ of\ shotcrete\ or\ floor\ slab = \ t_{sc\ or\ FS}\ L\ z\ \rho \tag{1b}$$

$$\text{Ejection area} = L\sum_1^n z_i \tag{1c}$$

where, Z represents the zone length at the opposite end of the depth of bulking material (obelisk), z corresponds to the zone length next to the excavation surface and n is the number of failed zones in the excavation surface as exemplified in Figure 2b for the right sidewall. The ejection area is the same for the back or floor and the right or left sidewall. As the notch deepens, Equation 1c is constant in the back or floor, but it steadily increases on the sidewalls.

2.5 *Kinetic energy flux*

The kinetic energy flux (E_k) per meter of tunnel can be calculated when the velocity of the sidewalls or back/floor is applied to the mass of the obelisk defined earlier as: $E_k = 0.5\ mass\ v^2$. The kinetic energy flux depicted in Figure 4 and Figure 5 is normalized by the ejection area.

The mass (m) includes both the obelisk and the layer of shotcrete or floor slab and $\boldsymbol{v}$ is the average velocity between the two grid points of the ejected obelisk as illustrated by Figure 2d. An example is presented by Figure 4. Moreover, Figure 5 depicts the scenario when the deepest depth of bulking in Figure 2b is ejected at the highest possible velocity, which is located at the excavation surface.

2.6 *Explicit inclusion of confining pressure*

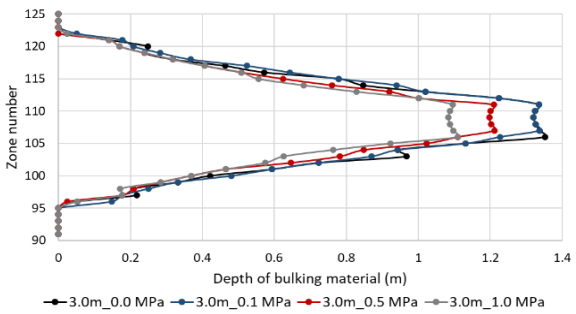

Figure 3. Effects of confining pressure suppressing axial and lateral extent of the depth of bulking material on the sidewalls of a 6 m wide tunnel.

The confining pressure is known to reduce the bulking factor (Kaiser 2016) as even small changes in the radial stress can reduce linear bulking and related displacements. FLAC facilitates the application of normal pressure to the excavation boundary. This approach uses confining pressure to qualitatively evaluate the effects of a well-connected areal support on rock stability and support demand. By this semi-empirical approach, the effect of confining pressure on the kinetic energy flux is investigated. The following support pressures are simulated: 0 MPa for unsupported tunnels and

0.1, 0.5, and 1 MPa for light support, heavy support, and a thick circular concrete liner, respectively. Figure 3 shows that as the confining pressure applied to the excavation boundary increases the depth of bulking material decreases whereas the lateral extent remains essentially constant.

3 RESULTS

3.1 Kinetic energy flux

Figure 4 depicts the distribution of kinetic energy flux normalized by the ejection area for four out of the six different geometries after progressive excavation of "failed material", without applying confining pressure. As the major axis of the resultant excavation is increased the displacement demand and related velocity at the excavation boundary along the horizontal axis, and therefore the energy flux for a constant bulking duration, increase (b), decrease (c) and then increases slightly (d).

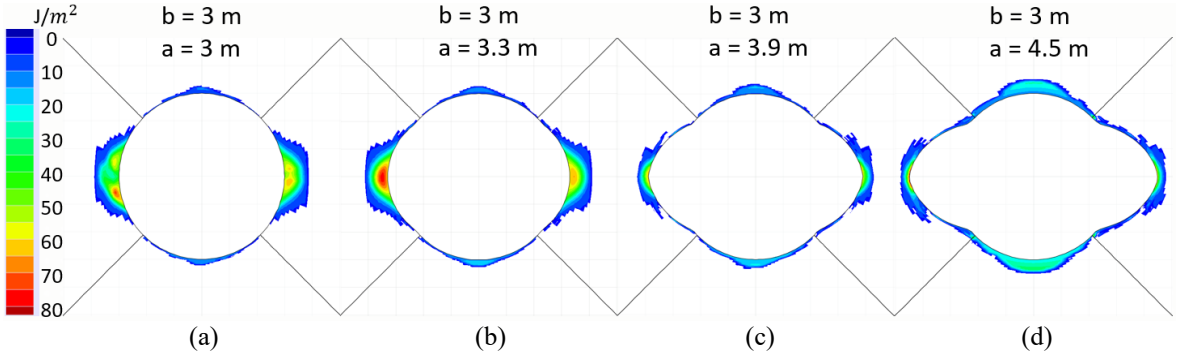

Figure 4. Kinetic energy (J/m2) demands around zones for four tunnel geometries, with a and b representing the semi-major and semi-minor axes, respectively.

Figure 4b represents a transitional case where the displacement demand and related velocity increase slightly at the excavation boundary (energy increase) before reducing (for more elliptical geometries as illustrated in Figure 4d) due to geometrically inherent confinement effects.

Note that the kinetic energy demand in the back and floor regions increases steadily when comparing geometries from (a) to (d). The highest kinetic energy demand is observed in the back and floor regions when a = 4.5, where more zones failed in tension (increasing the mass to be ejected) at a relatively higher ejection speed, due to an increase in the excavation span. This phenomenon, known as shape change, where rapid bulking on the sidewalls changes the excavation span, can cause an increasing kinetic energy demand in the back and floor regions as a function of the excavation span and can only be fully understood by utilizing the appropriate geometry in continuum models.

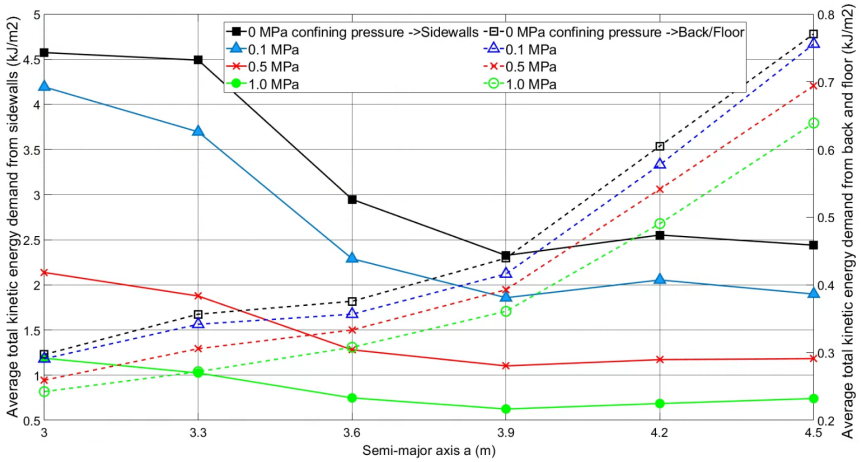

Figure 5. Average total kinetic energy (kJ/m2) demand from sidewalls and back and floor for the six proposed geometries with increasing semi-major axis a.

3.2 Summation of kinetic energy demand for the entire bulking volume (all obelisks)

The kinetic energy flux was estimated for six geometries considering the mass of shotcrete or floor slab, the mass of the obelisk at the deepest depth of bulking material and the highest possible velocity, which is located at the excavation surface, corresponding to the worst-case scenario of energy release. The total kinetic energy demand corresponds to the summation of all the largest possible obelisks within the failing zones. Figure 5 illustrates the average total kinetic energy demand normalized by the ejection area on the sidewalls and the back and floor as a function of the semi-major axis a.

The impact of confining pressure on reducing kinetic demand is more significant on the sidewalls than on the back and floor. Consequently, the kinetic energy flux due to rapid bulking on the sidewalls is always higher. Note that for an initially circular excavation, the kinetic energy demand on the back and floor is low compared to that on the sidewalls. However, as the excavation shape changes from circular to elliptical, for instance, for the case when the major axis a = 4.5 m, the kinetic energy demand on the back and floor can be up to 33%, 55% and even 90% for 0.1, 0.5 and 1 MPa of explicitly included support pressure, respectively, the kinetic energy demand on the sidewalls.

4 CONCLUSIONS

The relevance of shape change becomes evident from the estimated kinetic energy flux calculations. For this, the discontinuum nature of the brittle failure must be acknowledged and different geometries corresponding to different stages of progressive failure have to be considered. As the semi-major axis a increases, which corresponds to a rock mass that has experienced two-sided strainbursts, the kinetic energy demand on the back and floor approaches the demand on the sidewalls as the explicitly simulated support pressure increases.

The effects of rock support are simulated by surface pressure, and even though very complex to accurately quantify such pressure for different support designs, is demonstrated to reduce energy flux. The application of confining pressure via a well-connected rock support system does decrease the energy demand on the support. This is supported by the practical experience that robust areal support systems reduce damage in heavy bursting ground. Further studies should focus on the effects of rock reinforcement on displacement and kinetic energy demands.

5 REFERENCES

Diederichs, M. S. (2007). The 2003 Canadian Geotechnical Colloquium: Mechanistic interpretation and practical application of damage and spalling prediction criteria for deep tunnelling. *Canadian Geotechnical Journal*, *44*(9), 1082–1116.

Gonzalez, F. J., Kaiser, P. K., & Diederichs, M. S. (2022). Energy Release Resulting from Sudden Excavation Shape Changes during Two-sided Strainbursts. *In ISRM European Rock Mechanics Symposium-EUROCK 2022. OnePetro*.

Itasca Consulting Group Inc. (2019). *FLAC users' manual* [Version 8.10].

Kaiser, P. K. (2016). Constructability of Deep Underground Excavations – Challenges of managing highly stressed ground in civil and mining projects. *Sir Muir Wood Lecture of International Tunnelling Association at World Tunnelling Congress, San Francisco*, 33.

Kaiser, P. K., & Malovichko, D. (2022). Energy and displacement demands imposed on rock support by strainburst damage mechanisms. *Proceedings of the Tenth International Symposium on Rockburst and Seismicity in Mines (RaSiM10), Tucson, Arizona,United States*.

Kaiser, P. K., & Moss, A. (2021). Deformation-based support design for highly stressed ground with a focus on rockburst damage mitigation. *J. of Rock Mech. and Geotechnical Engineering*.

Malovichko, D. (2020). Description of seismic sources in underground mines: Theory. *Bulleting of the Seismological Society of America*, *110*(5), 2124–2137.

Martin, C. D., Read, R. S., & Martino, J. B. (1997). Bservations of brittle failure around a circular test tunnel. *Int. Journal of Rock Mechanics and Mining Sciences*, *34*(7), 1065–1073.